XVI International Conference on Durability of Building Materials and Components
DBMC 2023, China
K.F. Li and D.P. Fang (Eds)

Study of the Chemical Processes of Combined Sulfate-chloride Attack on Low-carbon Cementitious Materials

François El Inaty[1], Mario Marchetti[1], Marc Quiertant[2], Othman Omikrine-Metalssi[1]

[1]Univ Gustave Eiffel, Cerema, UMR MCD, F- 77454 Marne-la-Vallée, France, francois.el-inaty@univ-eiffel.fr (Francois El Inaty), othman.omikrine-metalssi@univ-eiffel.fr (Othman Omikrine-Metalssi), mario.marchetti@univ-eiffel.fr (Mario Marchetti)

[2]Univ Gustave Eiffel, EMGCU, F- 77454 Marne-la-Vallée, France, marc.quiertant@univ-eiffel.fr (Marc Quiertant)

Abstract. *In marine environments, concrete structures are not only exposed to sulfate ions but also to chloride ones, from an early age. This leads to concrete expansion and cracking as well as steel reinforcements corrosion. However, the coupling effect of sulfate and chloride is still not widely studied. When addressed, some researchers showed that chloride ions mitigate the effect of sulfate while others concluded that it accelerates it and vice versa. Therefore, one of the objectives of this study is to observe both the combined and individual effects of chloride on sulfate attack. The second objective is to perceive the resistance of selected additives (fly ash, blast furnace slag, and metakaolin) to a combined attack. Then, powders of pure cement, binary, ternary, and quaternary blended pastes were immersed in sulfate, chloride, and sulfate-chloride solutions at an early age. Results of the characterization showed that the ettringite formation was delayed due to the presence of chloride. However, the presence of sulfate ions accelerated the chloride effect. The incorporation of more than one additive enhanced the samples' durability.*

Keywords: *Durability; Sulfate; Chloride; Supplementary cementitious materials; Early age; Chemical alterations*

1 Introduction

One of the threats affecting Reinforced Concrete (RC) structures' durability is the External Sulfate Attack (ESA) (Jabbour et al., 2022; Ragoug et al., 2019). ESA occurs when RC structures are placed in an environment rich in sulfates such as seawater, groundwater, and some types of soils (Whittaker and Black, 2015). When sulfate ions penetrate the concrete matrix, they react with calcium hydroxide to form ettringite (Jabbour et al., 2022; Ragoug et al., 2019). Moreover, sulfates react with calcium silicates to form gypsum (El Inaty et al., 2022; Ran et al., 2022). Both ettringite and gypsum are expensive products that damage RC structures (Gu et al., 2022, 2019; Sahu and Thaulow, 2004). However, RC structures are often exposed to many chemical ions, at the same time, that alter their durability. For example, RC structures found in marine environments are not only exposed to sulfate ions but also chloride ions (Sun et al., 2022). Chloride ions, when not captured by the hydration products of cementitious materials as Friedel's salt, result in the dissolution of iron in RC structures (Neville, 1995). Stroh et al. have described the mechanisms of the coupled effects of sulfate and chloride attack (Stroh et al., 2016). They mentioned that chloride ions penetrate quickly into the concrete matrix to form Friedel's salt. After, sulfate ions form gypsum in the first place, and the excess of sulfate creates ettringite. Also, they found out that the presence of sulfate ions leads to the

destabilization of Friedel's salt. Many other studies (Dehwah et al., 2002; Geng et al., 2015; Mavropoulou et al., 2016) came to support the idea of the destabilization of Friedel's salt and the decrease of the chloride binding when sulfate is present and therefore showing that sulfate accelerates chloride ions' attack. However, other studies (Shaheen and Pradhan, 2017; Zuquan et al., 2007) contradicted this idea by showing that sulfate ions attenuate the chloride diffusion, by decreasing the porosity of concrete. Regarding the effect of chloride ions on the ESA, many researchers observed that chloride inhibited the effect of the sulfate attack (Baghabra Al-Amoudi, 2002; Lee et al., 2008). In contrast, experiments on the effect of chloride ions on ettringite formation are lacking (Ran et al., 2023). It is clear that the effect of chloride on sulfate and vice versa is a debatable subject and may be influenced by factors such as the type of cation used and the incorporated pozzolans (Ramezanianpour and Riahi Dehkordi, 2017).

Accordingly, this study aims to better understand the chemical effect of chloride ions on sulfate attack on cementitious materials and vice versa. It also investigates the durability of low-carbon cementitious materials in this respect. To reach those objectives, 15g of pure cement, binary, ternary, and quaternary blended pastes powder are exposed to chloride, sulfate, and chloride-sulfate solutions for 25 days. The characterization methods are based on Raman spectroscopy, thermogravimetric analysis, and Fourier-transform infrared spectroscopy.

2 Materials and Methods

2.1 Materials

The cement utilized in this study was a CEM I 52.5 N CE CP2 NF manufactured by EQIOM. The manufacturer provided information on its composition, which is listed in Table 1. Fly ash and blast furnace slag were also employed and their chemical composition is displayed in Table 1. In comparison to the other additives, the CEM I has the highest CaO content and the lowest Al_2O_3 and SiO_2 contents. Blast furnace slag also had a higher CaO content compared to fly ash. Moreover, BASF MetaMax metakaolin was also used in this study. According to the manufacturer, it was made out of 100% by weight of calcined kaolin.

Table 1. Chemical composition of the used materials.

Components	CEM I Wt (%)	Fly ash Wt (%)	Blast furnace slag Wt (%)
SiO_2	20.38	70.83	35.71
Al_2O_3	4.30	24.36	10.65
Fe_2O_3	3.80	2.24	0.45
TiO_2	0.24	1.48	0.73
MnO	0.08	0.05	0.23
CaO	62.79	0.06	43.32
MgO	1.25	0.23	3.97
SO_3	3.46	-	3.06
K_2O	0.73	0.64	0.45
Na_2O	0.35	0.1	0.16
P_2O_5	-	0.05	0.02
S^{2-}	traces	-	-
Cl^-	0.05	-	-
LOI*	2.54	-	-

Free lime	1.39	-	-

*loss of ignition

2.2 Mixes Design

Four mixes were utilized in this study. These mixes consisted of pure cement, binary, ternary, and quaternary blended pastes, all of which had varying supplementary cementitious materials and cement blends (Table 2). The selection of these formulations is grounded in a chemical composition criterion. This criterion is based on the evaluation of the ratio between calcium oxide and silicon, aluminium, and iron oxides, considering the standardized types of cement that are specified in NF EN 197-1 (European Committee for Standardization, 2011), which include CEM I, II, III, IV, and V types.

Table 2. Mixes design.

	CEMI	Blast furnace slag	Metakaolin	Fly Ash
Mix 1 (Reference)	100%	-	-	-
Mix 2	55%	45%	-	-
Mix 3	55%	35%	10%	-
Mix 4	55%	20%	10%	15%

2.3 Sampling and Exposure

For this study, prismatic specimens with dimensions of 40x40x160mm^3 were prepared using the four different mixes. The mixing process followed the guidelines of French standard NF EN 196-1 (NF 196-1, 2006). After 24 hours, the specimens were de-molded and crushed to a diameter inferior to 2.50mm at room temperature (22°C) to increase the surface exchange between the cementitious material and ions in the solutions. 15g of powder of each material was fully submerged in 120g of tap water, sulfate, chloride, and sulfate-chloride solutions, whose concentrations are presented in Table 3.

Table 3. The concentrations of sulfate and chloride ions in the exposure solutions.

	Sulfate	Chloride
EXP0 (tap water)	-	-
EXP1	-	30g/l
EXP2	15g/l	-
EXP3	15g/l	30g/l

2.4 Characterization Methods

2.4.1 Thermogravimetric analysis

The thermogravimetric analysis (TGA) technique was used to determine the chemical composition of the samples. The mass variation of the models was observed as a function of

temperature to identify the composition. The device used in the study was the NETZSCH STA 449 F1. The measurements were conducted under an inert nitrogen atmosphere, with a temperature range of 25 to 1250°C and a heating rate of 10°C per minute. The derivative of the thermogravimetric analysis curve (DTG) was obtained to identify the significant mass variations, such as losses or gains. For this method, powder samples were examined after 1, 2, 5, 11, 18, and 25 days of exposure. This enabled a more comprehensive understanding of the portlandite consumption due to chloride and sulfate attacks.

2.4.2 Fourier-transform infrared spectroscopy

The chemical composition of cementitious materials was characterized by FTIR spectroscopy using a Nicolet iS50 spectrometer, with a spectral range between 400 and 4000cm^{-1}. This qualitative method was used to identify chemical bonds in the tested materials. The obtained bands were compared to those found in the literature. The powders used for TGA were also utilized for spectroscopic measurements at room temperature (22°C). A comprehensive understanding of the chemical composition of the materials was then obtained. This was crucial for the analysis of the chemical effects of the coupling of chloride and sulfate ions.

2.4.3 Raman spectroscopy

Raman spectroscopy is a non-invasive technique employed for determining the chemical makeup of materials and even liquid solutions. The Raman spectrometer, a laser from BWTek operating with a 532nm laser (50mW), is adjusted and configured with the right laser and detector settings based on the sample properties. In this investigation, a specific immersion probe was implemented to examine the solutions through the sulfate ions consumption taking place during 1, 2, 5, 11, 18, and 25 days of the chemical attack.

3 Results and Discussion

3.1 Thermogravimetric Analysis

After being immersed in the four different solutions, TGA was performed on the four mixes at different ranges of time after being extracted from the solutions and dried for 24h at a temperature of 55 ± 5°C. According to previous research (Gao et al., 2022; Nochaiya et al., 2015), the first peak in the DTG curve, between 30°C and 200°C, indicates the decomposition of ettringite, C-S-H, and free water. Additionally, the presence of monosulfoaluminates (AFm) is indicated by a peak at 190°C. The dihydroxylation process of portlandite ($Ca(OH)_2$) causes the third peak between 450°C and 550°C, while the decarbonization of calcite ($CaCO_3$) results in the peak between 650°C and 820°C. For this study, portlandite losses were calculated and illustrated in Table 4. Also, AFm peaks were carefully observed. The reason behind this is that portlandite and AFm, in the presence of sulfate ions, participate in the formation of expensive products (Santhanam et al., 2002; Skaropoulou et al., 2013).
As shown in Table 4, all mixes, except Mix 1, exhibited a loss of portlandite when immersed in water, chloride, sulfate, or both chloride and sulfate. However, they were attacked at early age (hydration process is still in progress). The reason behind this loss is attributed to the portlandite consumption by chloride and sulfate. Moreover, the pozzolanic effect of Supplementary Cementitious Materials (SCMs) leads to a decrease in portlandite (Lothenbach

et al., 2011). Additionally, this method showed that when immersed in a sulfate solution, the portlandite consumption was more significant than in the other conditions. This indicates that the coupling of the two ions mitigated the attack. It is worth mentioning that the TGA method did not detect the presence of portlandite in mixes 4 and 5 (ternary and quaternary blended pastes).

AFm disappeared in the pastes that are subjected to only sulfate ions. Those results indicate that the presence of chloride and sulfate together significantly decreases the consumption of AFm and therefore the deterioration process of the cementitious materials.

Table 4. Portlandate consumption in Mixes 1 and 2 over time and at different exposure.

		Day 1	Day 2	Day 5	Day 11	Day 18	Day 25	D1 – D25
Mix 1	EXP0	3.92	5.08	5.19	4.82	5.54	5.68	-1.76
Mix 1	EXP1	3.9	4.69	3.82	3.96	4.4	4.89	-0.99
Mix 1	EXP2	3.53	3.93	3.7	3.2	2.85	3.32	0.21
Mix 1	EXP3	3.5	3.79	3.35	3.62	3.04	3.44	0.06
Mix 2	EXP0	2.28	2.05	1.78	1.91	1.75	1.96	0.32
Mix 2	EXP1	2.01	1.79	1.72	1.64	1.56	1.87	0.14
Mix 2	EXP2	1.67	1.43	1.1	1.06	1.09	0.91	0.76
Mix 2	EXP3	1.6	1.41	1.12	1.12	1.21	1.02	0.58

3.2 Fourier-transform Infrared Spectroscopy

FTIR analysis is a qualitative method that shows various absorption peaks that correspond to different functional groups existing in the tested material. According to previous studies (Farcas and Touzé, 2001; Liu et al., 2020; Yue et al., 2018), portlandite is typically found around 3642cm^{-1} coming from O-H stretching. Additionally, the band present at 1102 cm^{-1} corresponds to the S-O bond stretch from gypsum, ettringite, and monosulfoaluminates. Furthermore, the band observed at 610 cm^{-1} is associated with the S-O stretch of ettringite. Water can be detected by the broad band present at 3373cm^{-1}. Gypsum generates a band at 1680cm^{-1}, attributed to O-H stretching. The band observed at 1440 cm^{-1} indicates the presence of calcite and Friedel's salt, which can be identified by its C-O stretch. The band at approximately 967cm^{-1} corresponds to SiO_4 stretch, which can be attributed to C-S-H, calcium aluminate hydrates, and H_2O. Finally, Friedel's salt can be identified around 810 cm^{-1}.

Figure 1 provides insights into the performance of the tested mixes under different environmental conditions. Overall, minor differences were observed between the mixes. This was potentially due to the young age of the samples and the need for additional curing time especially for SCMs.

The peak at 3642cm^{-1}, where portlandite is present, revealed that the specie disappeared after one day of exposure to chloride in the first mix, after 18 days of exposure in the second mix and after 5 days of exposure in the third mix. This may be attributed to the low concentration of portlandite in these mixes, as found in the previous section. On the peak at 1685cm^{-1}, where gypsum can be found, the peak was consistently present in all mixes due to the presence of gypsum in the pastes. The peak at 1102cm^{-1} was observed in all mixes when sulfate was present,

suggesting the formation of gypsum and ettringite resulting from the chemical reaction between the hydrated products and sulfate ions.

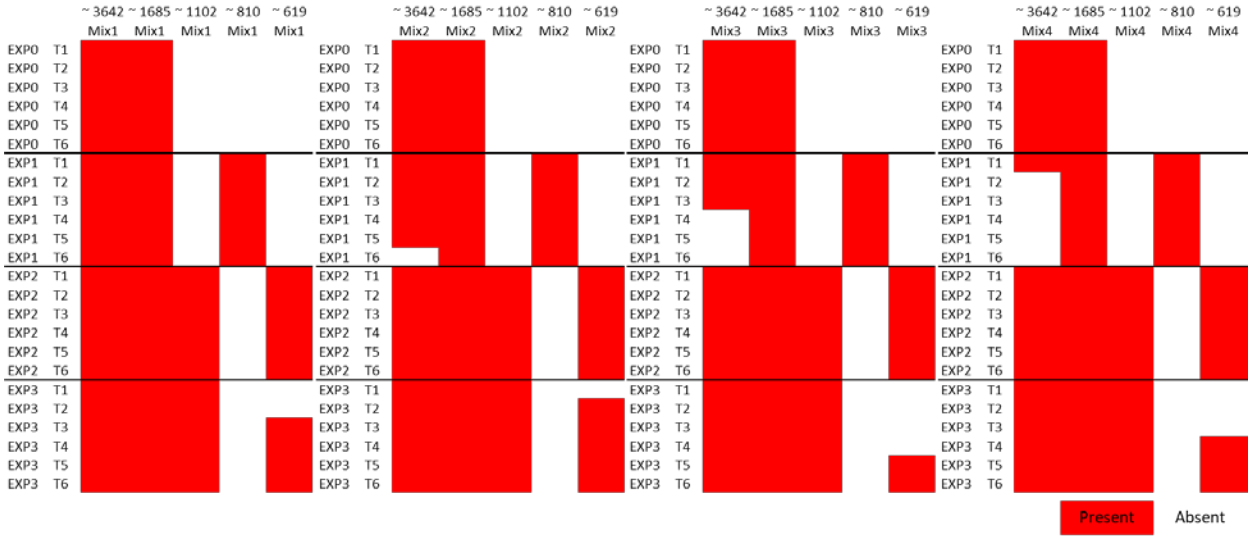

Figure 1. Different functional groups existing in the tested material influenced by different exposure environments and exposure durations.

The peak at 810cm^{-1} was only present when the mixes were exposed to chloride, indicating the presence of Friedel's salt. This suggests that in the presence of sulfate and chloride ions, the hydrated products did not cap the chloride ions, allowing them to remain free, and indicating that sulfate accelerated the chloride ion attack.

The peak at 619cm^{-1}, attributed to ettringite, was present in all mixes when only exposed to sulfate. However, it was retarded in the presence of both sulfate and chloride. The peak appeared after 3 days of exposure of Mix 1, one day of exposure of Mix 2, 18 days of exposure of the third mix, and 11 days of exposure of the fourth one. These results were correlated with the ATG test, which indicated that the presence of chloride mitigated the sulfate ion attack.

The comparison between the four mixes in terms of chemical reactions was difficult, as they were attacked at a young age before completion of the hydration process. However, the incorporation of more than one SCM (Mixes 3 and 4) appeared to delay the ettringite formation.

3.3 Raman Spectroscopy

In this study, Raman spectroscopy was utilized to assess the depletion of sulfate ions in the test solutions. The vibrational mode of SO_4^{2-} was detected around the 1000cm^{-1} region, which is characteristic of sulfate (Tang et al., 2021). The results indicated that the sulfate ions available in the solution were not fully consumed even after a 25-day exposure period. In contrast, the reference mix (100% CEMI) showed complete sulfate depletion after only 11 days of exposure to the sulfate-only solution. This finding suggests that chloride ions may have contributed to mitigating the effect of sulfate ions, and that the blends containing SCMs demonstrated improved resistance to chemical attacks.

3.4 Discussion

The results of the ATG test indicated that portlandite was significantly consumed in the presence of sulfate ions. Moreover, under the same exposure condition, AFm was entirely consumed, as indicated by the FTIR results that demonstrated the significant formation of ettringite when solely exposed to sulfate. Chloride mitigated the sulfate attack. This finding can be also correlated with the consumption of sulfate ions in the sulfate-only solution as monitored by the Raman spectroscopy on sulfate solution.

The FTIR results showed the presence of Friedel's salt only in the mixes exposed to chloride, also, indicated a consumption of portlandite. The presence of sulfate with chloride accelerates the chloride ion diffusion due to the absence of bound chloride ions.

Although there were no significant differences between the mixes in terms of chemical reactions, incorporating more than one SCM delayed the formation of ettringite. This improved the mixes' resistance to attacks.

The characterization of the chemical changes induced by sulfate and chloride exposure in these low carbon cementitious powders has laid a solid foundation for understanding the behavior of these ions in the chemical alteration of cement-based materials. However, it is imperative to broaden the scope of investigation to encompass larger solid samples in order to uncover the physicochemical effects of sulfate and chloride within a complex matrix, simulating the conditions encountered in field situations. One fundamental aspect that demands attention is the transfer properties governing the diffusion and the migration of sulfate and chloride ions within the cement matrix. These transfer properties play a pivotal role in determining to what extent ions penetrate the matrix, their interaction with hydration products, and the resultant chemical changes affecting the properties themselves.

4 Conclusion

The objective of this investigation was to better understand the chemical reactions resulting from the coupling effect of chloride and sulfate ions on cementitious materials. In addition, the effectiveness of SCM blends was evaluated using pure cement, binary, ternary, and quaternary pastes. To achieve this, powders, extracted from the pastes, were subjected to different environments and compared. Based on the obtained results, the following conclusions can be drawn:

- When exposed to only sulfate, a significant consumption of portlandite and AFm was observed and an important formation of ettringite was recorded. Also, a complete depletion of sulfate ions was found in the solution. This shows that the presence of chloride along with sulfate ions mitigates the ESA.
- The formation of Friedel's salt and portlandite consumption were detected using the FTIR method, in the presence of chloride alone. However, this was not observed when coupling sulfate and chloride. This indicates that the presence of sulfate accelerates the chloride ions attack by preventing the bonding of free chloride ions.
- Incorporating more than one SCM delayed the ettringite formation and improved the mixes' resistance to attacks.

Further work should be done on the coupled effect of sulfate and chloride by incorporating also the physical process along with the chemical one on low carbon cementitious materials.

References

Baghabra Al-Amoudi, O.S., 2002. Attack on plain and blended cements exposed to aggressive sulfate environments. Cement and Concrete Composites 24, 305–316.

Dehwah, H.A.F., Maslehuddin, M., Austin, S.A., 2002. Long-term effect of sulfate ions and associated cation type on chloride-induced reinforcement corrosion in Portland cement concretes. Cement and Concrete Composites, CORROSION AND CORROSION MONITORING 24, 17–25.

El Inaty, F., Baz, B., Aouad, G., 2022. Long-term durability assessment of 3D printed concrete. Journal of Adhesion Science and Technology 0, 1–16.

European Committee for Standardization, 2011. EN 197-1:2011 Cement—Part 1: Composition, specifications and conformity criteria for common cements.

Farcas, F., Touzé, P., 2001. La spectrométrie infrarouge à transformée de Fourier (IRTF) 12.

Gao, Y., Cui, X., Lu, N., Hou, S., He, Z., Liang, C., 2022. Effect of recycled powders on the mechanical properties and durability of fully recycled fiber-reinforced mortar. Journal of Building Engineering 45, 103574.

Geng, J., Easterbrook, D., Li, L., Mo, L., 2015. The stability of bound chlorides in cement paste with sulfate attack. Cement and Concrete Research 68, 211–222.

Gu, Y., Dangla, P., Martin, R.-P., Omikrine Metalssi, O., Fen-Chong, T., 2022. Modeling the sulfate attack induced expansion of cementitious materials based on interface-controlled crystal growth mechanisms. Cement and Concrete Research 152, 106676.

Gu, Y., Martin, R.-P., Omikrine Metalssi, O., Fen-Chong, T., Dangla, P., 2019. Pore size analyses of cement paste exposed to external sulfate attack and delayed ettringite formation. Cement and Concrete Research 123, 105766.

Jabbour, M., Metalssi, O.O., Quiertant, M., Baroghel-Bouny, V., 2022. A Critical Review of Existing Test-Methods for External Sulfate Attack. Materials 15, 7554.

Lee, S.-T., Park, D.-W., Ann, K.-Y., 2008. Mitigating effect of chloride ions on sulfate attack of cement mortars with or without silica fume. Can. J. Civ. Eng. 35, 1210–1220.

Liu, P., Chen, Y., Wang, W., Yu, Z., 2020. Effect of physical and chemical sulfate attack on performance degradation of concrete under different conditions. Chemical Physics Letters 745, 137254.

Lothenbach, B., Scrivener, K., Hooton, R.D., 2011. Supplementary cementitious materials. Cement and Concrete Research, Conferences Special: Cement Hydration Kinetics and Modeling, Quebec City, 2009 & CONMOD10, Lausanne, 2010 41, 1244–1256.

Mavropoulou, N., Katsiotis, N., Giannakopoulos, J., Koutsodontis, K., Papageorgiou, D., Chaniotakis, E., Katsioti, M., Tsakiridis, P.E., 2016. Durability evaluation of cement exposed to combined action of chloride and sulphate ions at elevated temperature: The role of limestone filler. Construction and Building Materials 124, 558–565.

Neville, A., 1995. Chloride attack of reinforced concrete: an overview. Materials and Structures 28, 63–70.

NF 196-1, 2006. Méthodes d'essais des ciments.

Nochaiya, T., Sekine, Y., Choopun, S., Chaipanich, A., 2015. Microstructure, characterizations, functionality and compressive strength of cement-based materials using zinc oxide nanoparticles as an additive. Journal of Alloys and Compounds 630, 1–10.

Ragoug, R., Metalssi, O.O., Barberon, F., Torrenti, J.-M., Roussel, N., Divet, L., d'Espinose de Lacaillerie, J.-B., 2019. Durability of cement pastes exposed to external sulfate attack and leaching: Physical and chemical aspects. Cement and Concrete Research 116, 134–145.

Ramezanianpour, A.A., Riahi Dehkordi, E., 2017. Effect of Combined Sulfate-Chloride Attack on Concrete Durability-A Review. AUT Journal of Civil Engineering 1, 103–110.

Ran, B., Li, K., Fen-Chong, T., Omikrine-Metalssi, O., Dangla, P., 2022. Spalling rate of concretes subject to combined leaching and external sulfate attack. Cement and Concrete Research 162, 106951. https://doi.org/10.1016/j.cemconres.2022.106951.

Ran, B., Omikrine-Metalssi, O., Fen-Chong, T., Dangla, P., Li, K., 2023. Pore crystallization and expansion of cement pastes in sulfate solutions with and without chlorides. Cement and Concrete Research 166, 107099.

Sahu, S., Thaulow, N., 2004. Delayed ettringite formation in Swedish concrete railroad ties. Cement and Concrete Research, H. F. W. Taylor Commemorative Issue 34, 1675–1681.

Santhanam, M., Cohen, M.D., Olek, J., 2002. Mechanism of sulfate attack: A fresh look: Part 1: Summary of experimental results. Cement and Concrete Research 32, 915–921.

Shaheen, F., Pradhan, B., 2017. Influence of sulfate ion and associated cation type on steel reinforcement corrosion in concrete powder aqueous solution in the presence of chloride ions. Cement and Concrete Research 91, 73–86.

Skaropoulou, A., Sotiriadis, K., Kakali, G., Tsivilis, S., 2013. Use of mineral admixtures to improve the resistance of limestone cement concrete against thaumasite form of sulfate attack. Cement and Concrete Composites 37, 267–275.

Stroh, J., Meng, B., Emmerling, F., 2016. Deterioration of hardened cement paste under combined sulphate-chloride attack investigated by synchrotron XRD. Solid State Sciences 56, 29–44.

Sun, D., Cao, Z., Huang, C., Wu, K., De Schutter, G., Zhang, L., 2022. Degradation of concrete in marine environment under coupled chloride and sulfate attack: A numerical and experimental study. Case Studies in Construction Materials 17, e01218.

Tang, C., Ling, T.-C., Mo, K.H., 2021. Raman spectroscopy as a tool to understand the mechanism of concrete durability—A review. Construction and Building Materials 268, 121079.

Whittaker, M., Black, L., 2015. Current knowledge of external sulfate attack. Advances in Cement Research 27, 532–545.

Yue, Y., Wang, J.J., Basheer, P.A.M., Bai, Y., 2018. Raman spectroscopic investigation of Friedel's salt. Cement and Concrete Composites 86, 306–314.

Zuquan, J., Wei, S., Yunsheng, Z., Jinyang, J., Jianzhong, L., 2007. Interaction between sulfate and chloride solution attack of concretes with and without fly ash. Cement and Concrete Research 37, 1223–1232.